

Cite this: *Phys. Chem. Chem. Phys.*, 2011, **13**, 4596–4599

www.rsc.org/pccp

PAPER

Nanoscale changes induce microscale effects in Turing patterns

Jorge Carballido-Landeira,^a Pablo Taboada^b and Alberto P. Muñuzuri^a

Received 2nd November 2010, Accepted 1st December 2010

DOI: 10.1039/c0cp02362k

A water-in-oil microemulsion loaded with a reaction-diffusion chemical system (Belousov-Zhabotinsky reaction) is able to exhibit Turing patterns that are believed to be responsible for differentiation processes in Nature. Using polymers, such as polyethylene oxide, longer than the droplet size changes the distribution of droplets due to cluster formation. This difference in the nanoscale has relevant consequences in the observed Turing pattern's wavelength, which is three orders of magnitude larger than the droplet size.

1. Introduction

Pattern formation in systems far from equilibrium has played an important role in different scientific areas such as biology¹ and non-linear chemistry.^{2,3} An example of a chemical reaction-diffusion system that exhibits a diversity of non-monotonic behaviors is the Belousov-Zhabotinsky (BZ) reaction⁴ confined in water-in-oil (w/o) microemulsions, where AOT (sodium bis(2-ethylhexyl)sulfosuccinate) is frequently used as the stabilizing amphiphile.^{5–7} On changing the confinement conditions where the BZ reaction takes place,⁸ the BZ-AOT system is able to present different dynamics, ranging from Turing structures^{9,29} to standing waves¹⁰ and packet waves.¹¹ Characteristic parameters defining the properties of the AOT reverse microemulsion such as the droplet radius and the droplet volume fraction^{12–14} appear as relevant factors to regulate the formation of patterns.⁸

In this regard, formation of droplet clusters and subsequent percolation phenomena, in which individual spherical droplets and droplet clusters transform into elongated water channels and induce changes of several orders of magnitude in both viscosity and electrical conductivity,^{15,16} should affect pattern formation, its features and dynamics. In this regard, temperature has been shown to be a means for percolation to appear.¹⁷ Thus, by using the temperature as an external forcing of BZ-AOT systems under different initial conditions a variety of spatiotemporal structures whose dynamics differ from the room temperature pattern was found.^{18–20} Clusters of droplets have also been obtained due to the ability of reverse microemulsions to host different hydrophilic macromolecules such as enzymes^{21–23} or polymers.^{24–26} Polymer-induced cluster formation and percolation has been shown to depend on the relation between the polymer chain length and the nanodroplet radius.²⁷ In particular, the homopolymer polyethylene oxide (PEO) was

proposed as a model macromolecule to better establish the interactions between droplets in reverse microemulsions²⁸ and, also, to understand and control the percolation phenomenon.

Here, we report on the control of the characteristic features of Turing patterns formed following a BZ reaction confined in an AOT-water-octane (w/o) microemulsion system by modifying the PEO concentration in the reaction medium. We observed that with small increasing concentrations of the homopolymer in the microemulsion we induced severe changes in its structure, that is, the formation of polymer-induced droplet clusters. These changes in the microemulsion structure involve dramatic modifications in the features of the Turing patterns formed in the absence and in the presence of the homopolymer in solution, which are related to variations of the diffusion coefficients of the species present in solution.

In a previous paper, we reported on the effect of PEO of different molecular weights with chain sizes shorter than the droplet radius in a BZ-AOT system. We observed remarkable differences in the characteristic lengths of the dashed wave patterns formed.³⁰ In this case, travelling waves breaking into segments could be observed for 24 h, while polymer-stabilized droplets maintained constant their hydrodynamic radii. Therefore, a detailed knowledge about the conditions at which the BZ reaction confined in the AOT reverse microemulsion system is necessary in order to achieve full control on the type and characteristics of the generated spatio-temporal patterns.

2. Experimental

All chemicals were purchased from Sigma-Aldrich Chemical Co and used as received, except octane that was purified by mixing with concentrated H₂SO₄ for 2 days.

In a typical sample preparation, a solution of 1.5 M AOT in octane was used to make two different AOT microemulsions (MEs) with different aqueous content. The first microemulsion (ME₁) was composed of malonic acid (MA) and H₂SO₄, while the second one (ME₂) was loaded with a 25 mM ferroin

^a Group of Nonlinear Physics, Universidade de Santiago de Compostela, Santiago de Compostela, E-15782, Spain

^b Colloids and Polymers Physics Group, Universidade de Santiago de Compostela, Santiago de Compostela, E-15782, Spain

solution and bromate. Ferroin was elaborated in our laboratory as a solution of 1 M FeSO₄ and 3 M of 1, 10-Phenanthroline. The homopolymer PEO ($M_w = 35\,000\text{ g mol}^{-1}$, named as PEO 35000) was diluted at the desired concentrations into the aqueous phase of both microemulsions, prior the addition of AOT in octane. The resultant microemulsion was obtained mixing equal volumes of both MEs and diluting with octane.

Dynamic light scattering measurements were performed with a laser light scattering instrument with vertically polarized incident light ($\lambda = 488\text{ nm}$, 2 W argon ion laser, Coherent Inc., Santa Clara, CA) combined with a digital correlator (ALV 5000E, ALV GmbH, Germany). All solutions were previously filtered (0.2 μm cellulose nitrate membranes, Whatman[®] GmbH, Dassel, Germany). DLS correlation data were analyzed by the constrained regularized CONTIN method to obtain distributions of decay rate.^{31,32} The hydrodynamic radius r_h was estimated from the diffusion coefficient using the Stokes–Einstein equation and assuming that the solvent viscosity is that of octane

$$D_0 = k_B T / 6\pi\eta r_h \quad (1)$$

where D_0 is the diffusion coefficient of a sphere at infinite dilution, k_B the Boltzmann constant, T the absolute temperature, and η the solvent viscosity.

Electrical conductivity measurements were performed using a Mettler Toledo SevenEasy Conductivity meter at room temperature using an inLab 730 measuring cell.

In order to image the spatio-temporal patterns, a drop of the resultant microemulsion was sandwiched between two transparent windows separated by a Teflon spacer (Zeflour membrane) of 80 μm . To observe pattern formation, we used a camera (Guppy AVT 64 fps) with an achromatic objective (DIN 4 \times Edmund Optics) connected to a personal computer.

3. Results

Initial conditions of active media were kept constant to analyze the effect of polymer PEO 35000 on pattern formation. In this way, the concentration of BZ reactants in the aqueous phase were: $[\text{MA}]_0 = 0.25\text{ M}$, $[\text{H}_2\text{SO}_4]_0 = 0.17\text{ M}$, $[\text{NaBrO}_3]_0 = 0.16\text{ M}$, and $[\text{ferroin}]_0 = 4\text{ mM}$. The concentration of droplets was determined by means of the volume fraction of the dispersed phase ($\varphi_d = 0.36$), while the droplet size was obtained through the relation $\omega \equiv [\text{H}_2\text{O}]/[\text{AOT}] = 18$.³³ Experiments were made by changing the polymer to water molar ratio, P ($P = [\text{PEO}]/[\text{H}_2\text{O}]$). We restricted our analysis to P values lower than 2.4 as a consequence of phase separation at larger P values.

The BZ-AOT system under the above chemical conditions, both in the absence and in the presence of PEO 35000, exhibits Turing structures³⁴ after several bulk oscillations (Fig. 1a). These patterns remained steady for one hour occupying the entire reactor and, then, slowly fade away. The characteristic wavelength of these Turing patterns was analyzed through two-dimensional FFT (see insets in Fig. 1a–1c). It was observed that patterns change under the presence of varying concentrations of PEO 35000 (see Fig. 1). Fig. 1d shows the progressive decrease of characteristic dimensionless wavelength, $\lambda = \lambda_{\text{PEO}}/\lambda_0$ (ratio between the wavelength in presence,

λ_{PEO} , and in absence, λ_0 , of polymer), of the Turing patterns with increasing P ratio. Values up to half of the characteristic pattern wavelength in the absence of homopolymer were reached.

In order to elucidate whether the changes in Turing pattern features are related to changes in microemulsion nanostructure, we performed DLS measurements for the BZ-AOT microemulsion system in both the absence and the presence of different homopolymer concentrations. It is necessary to point out that these experiments were made in the absence of ferroin in order to avoid solution coloration. In the absence of polymer, the droplet size distribution observed involves the presence of a main peak centered at *ca.* 5 nm (see Fig. 2a), in fair agreement with the droplet size predicted by using the well-known approximated relation $R = 0.175\omega$ ($r_h = 3.5\text{ nm}$).³⁵ In addition, a very small second peak can also be observed corresponding to mean sizes one order of magnitude larger than the former one. This may indicate the presence of a little portion of aggregated water droplets. In contrast, when the PEO polymer is added ($P = 2.4$ in Fig. 2a, as an example), a dramatic change in both mean droplet sizes and population distribution profiles are observed: Regarding droplet size values, we observe that the peak corresponding to individual droplets decreases in magnitude and also broadens, but the mean droplet size remains almost unaltered (*ca.* $r_h = 5\text{ nm}$). Nevertheless, the second peak largely increases in intensity and also shifts to larger size values, thus confirming the formation of droplet clusters. In other words, the two displayed peaks would correspond to two well-differentiated relaxation modes in the intensity correlation function:³⁶ the first one associated to droplet self-diffusion and the second one to collective diffusion of the associated water droplets.^{37,38}

By using the Stokes–Einstein equation, we express the effect of polymer on microemulsion structure in terms of diffusion coefficients. Thus, we define D_s and D_f as the slow and fast diffusion coefficient corresponding to clustered and single droplets, respectively. Dimensionless units were used to clearly

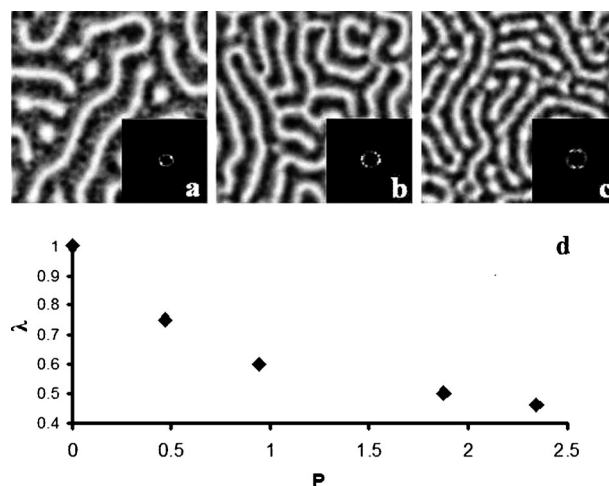


Fig. 1 Turing structures observed in a BZ-AOT system for different $P = [\text{PEO}]/[\text{H}_2\text{O}]$. Ratios: (a) $P = 0$, (b) $P = 0.9$ and (c) $P = 2.4$. Insets are the 2D Fourier spectra of the respective pattern images. Frame sizes are $1.3 \times 1.3\text{ mm}$. (d) Variation of the non-dimensional Turing wavelength with polymer concentration.

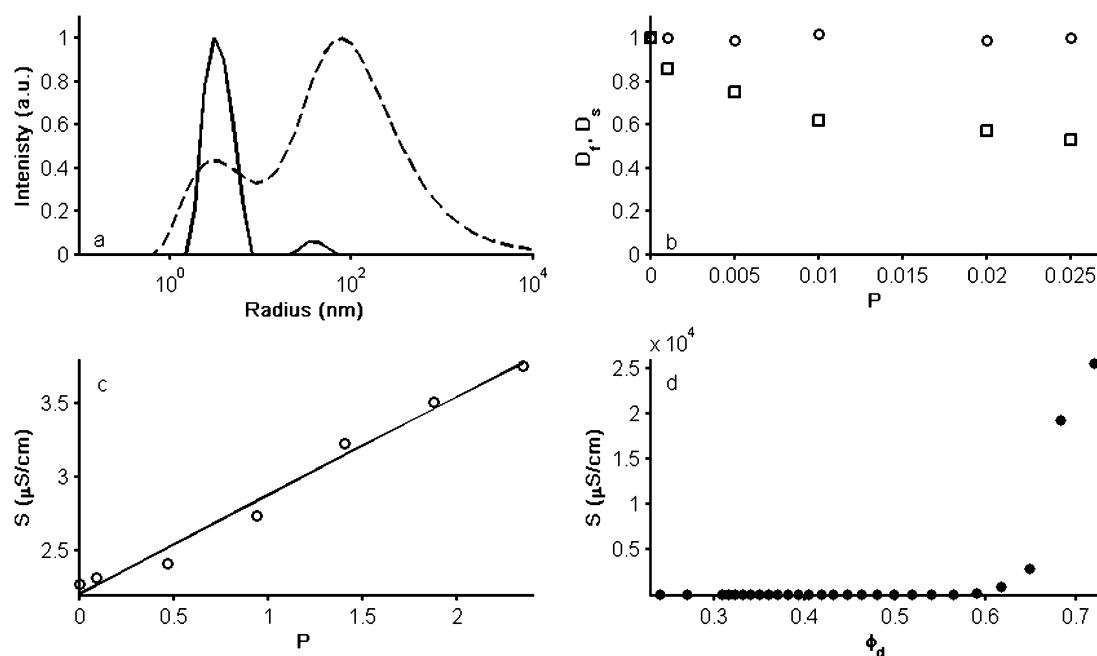


Fig. 2 (a) Droplet size distribution expressed in terms of hydrodynamic radius, r_h , of the BZ-AOT system for two different polymer concentrations: $P = 0$ (solid line) and $P = 2.4$ (dashed line). (b) Variation of the dimensionless diffusion coefficients (\circ) fast mode and (\square) slow mode with polymer concentration. (c) Dependence of electrical conductivity with polymer concentration (P) for the BZ-AOT system at fixed $\phi_d = 0.36$. (d) Variation of the electrical conductivity with the volume fraction of the dispersed phase (ϕ_d) for the AOT microemulsion loaded with the BZ reaction.

show the variation of the diffusion modes when the polymer is present in the reactive system ($D_1 = D_s/D_{s0}$ and $D_2 = D_f/D_{f0}$, with $D_{s0} = 10^{-11} \text{ m}^2 \text{ s}^{-1}$ and $D_{f0} = 1.4 \times 10^{-10} \text{ m}^2 \text{ s}^{-1}$ being the slow and fast diffusion coefficients of the BZ-AOT microemulsion system in the absence of PEO 35000). Fig. 2b shows the correlation between dimensionless diffusion coefficients (D_1 and D_2) and P . This plot reflects the constancy of the fast diffusion mode, whereas the slow mode monotonically decreases as P increases. Thus, changes in the characteristic patterns of the reactive BZ-AOT system seem to be related to changes in the microemulsion nanostructure.

Additional techniques were required to additionally confirm the nature of the population distribution corresponding to larger sizes in order to definitely ensure whether the percolation threshold was reached or, instead, polymer-induced droplet-clusters were obtained. Electrical conductivity measurements reveal a conductivity increase proportional to the added homopolymer concentration (Fig. 2c); nevertheless this increase is rather below the four orders of magnitude conductivity rises once the percolation is reached in the AOT system loaded with the BZ reaction (Fig. 2d).¹⁶ This result seems to confirm that our BZ-AOT system is below the percolation threshold for the polymer concentration range analyzed, and it is in good agreement with former predictions on Turing instability appearance in the microemulsion in the absence of polymer.⁸

4. Conclusions

In this paper we have studied experimentally the relation between Turing patterns features and microemulsion structure

in which the BZ reaction is confined. These changes in the BZ-reaction confinement in the AOT reverse microemulsion system in the nanometre scale have relevant effects in the microscale where Turing patterns are observed. From the experimental point of view, the use of a polymer with a mean chain size larger than the droplet size induces cluster formation and then, the appearance of a collective diffusion mode. A relationship between the size of confinement medium (or its corresponding diffusion coefficient) and the wavelength of these structures is also observed. This shortening in Turing wavelength was observed up to half of the value obtained for usual BZ-AOT and was delimited by phase separation for higher concentrations of the homopolymer.

The results here presented may be relevant for different fields in science as BZ-AOT system is considered a paradigm for pattern formation in a compartmented system. Most of the living systems that exhibit pattern formation in a spontaneous way are not continuously distributed but rather the active part is confined to a discrete distribution of cells. Thus, our results here may help in understanding the influence of the discrete structure inherent to life on the macroscopic observable patterns.

Acknowledgements

The authors thank MICINN by funding through research projects MAT2010-17336, FIS2007-64698 and FIS2010-21023 and Xunta de Galicia through projects INCITE09206020PR and PGIDIT06PXIB206169PR. J.C.L. also thanks MICINN by his FPI grant.

References

- 1 A. Gierer and H. Meinhardt, *Biol. Cybernetics*, 1972, **12**, 30–39.
- 2 R. J. Field and M. Burger, *Oscillations and Travelling Waves in Chemical Systems*, Wiley, New York, 1985.
- 3 I. R. Epstein and J. A. Pojman, *An Introduction to Nonlinear Chemical Dynamics*, Oxford University Press, Oxford U.K., 1998.
- 4 A. M. Zhabotinsky, *Proc. Acad. Sci.*, 1964, **157**, 392.
- 5 T. K. De and A. Maitra, *Adv. Colloid Interface Sci.*, 1995, **59**, 95.
- 6 D. Balasubramanian and G. A. Rodley, *J. Phys. Chem.*, 1988, **92**, 5995.
- 7 V. K. Vanag and I. Hanazaki, *J. Phys. Chem.*, 1995, **99**, 6944.
- 8 I. R. Epstein and V. Vanag, *Chaos*, 2005, **15**, 047510.
- 9 V. Vanag and I. R. Epstein, *Phys. Rev. Lett.*, 2001, **87**, 228301.
- 10 A. Kaminaga, V. Vanag and I. R. Epstein, *Phys. Rev. Lett.*, 2005, **95**, 058302.
- 11 V. Vanag and I. R. Epstein, *Phys. Rev. Lett.*, 2002, **88**, 088303.
- 12 J. Lang, A. Jada and A. Malliaris, *J. Phys. Chem.*, 1988, **92**, 1946–1953.
- 13 P. L. Lusi and B. Straub, *Structure and Reactivity in Reverse Micelles*, Plenum Press, London, 1984.
- 14 M. P. Pileni, *Structure and Reactivity in Reverse Micelles*, Elsevier, Amsterdam, 1989.
- 15 L. J. Schwartz, C. L. DeCiantis, S. Chapman, B. K. Kelley and J. P. Hornak, *Langmuir*, 1999, **15**, 5461.
- 16 H. Mays, *J. Phys. Chem. B*, 1997, **101**, 10271–10280.
- 17 Y. Feldman, N. Kozlovich, I. Nido and N. Garti, *J. Phys. Chem.*, 1996, **100**, 3745–3748.
- 18 R. E. McIlwaine, V. K. Vanag and I. R. Epstein, *Phys. Chem. Chem. Phys.*, 2009, **11**, 1581–1587.
- 19 A. Cherkashin, V. K. Vanag and I. R. Epstein, *J. Chem. Phys.*, 2008, **128**, 204508.
- 20 J. Carballido-Landeira, V. K. Vanag and I. R. Epstein, *Phys. Chem. Chem. Phys.*, 2010, **12**, 3656.
- 21 J. P. Huruguen, M. Authier, J. L. Greffe and M. Pileni, *Langmuir*, 1991, **7**, 243.
- 22 P. L. Luisi, M. Giomini, M. Pileni and B. H. Robinson, *Biochim. Biophys. Acta*, 1988, **947**, 209.
- 23 C. A. T. Laia and S. M. M. Costa, *J. Phys. Chem. B*, 2004, **108**, 7188–7197.
- 24 D. Papoutsis, P. Lianos and W. Brown, *Langmuir*, 1994, **10**, 3402–3405.
- 25 A. M. Belloccq, *Prog. Colloid Polym. Sci.*, 1997, **105**, 290–293.
- 26 M. J. Suarez, H. Levy and J. Lang, *J. Phys. Chem.*, 1993, **97**, 9808–9816.
- 27 C. Laia, W. Brown, M. Almgren and S. M. B. Costa, *Langmuir*, 2000, **16**, 465–470.
- 28 W. Meier, *Langmuir*, 1996, **12**, 1188–1192.
- 29 A. Kaminaga, V. K. Vanag and I. R. Epstein, *Angew. Chem. Int. Ed.*, 2006, **118**, 3159.
- 30 J. Carballido-Landeira, I. Berenstein, P. Taboada, V. Mosquera, V. K. Vanag, I. R. Epstein, V. Pérez-Villar and A. P. Muuzuri, *Phys. Chem. Chem. Phys.*, 2008, **10**, 1094–1096.
- 31 S. W. Provencher and P. Stepanek, *Part. Part. Syst. Charact.*, 1996, **13**(5), 291–294.
- 32 P. Stepanek and S. W. Provencher, *Macromol. Symp.*, 2000, **162**, 191–203.
- 33 M. P. Pileni, T. Zemb and C. Petit, *Chem. Phys. Lett.*, 1985, **118**, 414.
- 34 A. M. Turing, *Philos. Trans. R. Soc. London, Ser. B*, 1952, **237**, 37.
- 35 V. K. Vanag, *Phys.-Usp.*, 2004, **47**, 923–941.
- 36 A. Shukla, H. Graener and R. H. N. Neubert, *Langmuir*, 2004, **20**, 8526–8530.
- 37 M. B. Weissman, *J. Chem. Phys.*, 1980, **72**, 231.
- 38 P. N. Pusey, H. M. Fijnaut and A. Vrij, *J. Chem. Phys.*, 1982, **77**, 4270.